University of Wollongong

Research Online

1-1-2009

Effect of pre-straining and bake hardening on the microstructure and mechanical properties of CMnSi TRIP steels

L. C. Zhang
laichang@uow.edu.au

I. B. Timokhina
Monash University, Ilana.Timokhina@eng.monash.edu.au

A. La Fontaine
The University of Sydney

S. P. Ringer
University of Sydney

P. D. Hodgson
Deakin University

See next page for additional authors

Follow this and additional works at: https://ro.uow.edu.au/engpapers

Part of the Engineering Commons

https://ro.uow.edu.au/engpapers/507

Recommended Citation

Authors

L. C. Zhang, I. B. Timokhina, A. La Fontaine, S. P. Ringer, P. D. Hodgson, and E V. Pereloma

EFFECT OF PRE-STRAINING AND BAKE HARDENING ON THE MICROSTRUCTURE AND MECHANICAL PROPERTIES OF CMnSi TRIP STEELS

L.C. Zhang, I.B. Timokhina, A. La Fontaine, S.P. Ringer, P.D. Hodgson, E.V. Pereloma

The effects of pre-straining and bake hardening on the mechanical behaviour and microstructural changes were studied in two CMnSi TRansformation-Induced Plasticity (TRIP) steels with different microstructures after intercritical annealing. The TRIP steels before and after pre-straining and bake hardening were characterised by X-ray diffraction, optical microscopy, transmission electron microscopy, three dimensional atom probe and tensile tests. Both steels exhibited discontinuous yielding behaviour and a significant strength increase with some reduction in ductility after pre-straining and bake hardening treatment. The following main microstructural changes are responsible for the observed mechanical behaviours: a decrease in the volume fraction of retained austenite, an increase in the dislocation density and the formation of cell substructure in the polygonal ferrite, higher localized dislocation density in the polygonal ferrite regions adjacent to martensite or retained austenite, and the precipitation of fine iron carbides in bainite and martensite. The mechanism for the observed yield point phenomenon in both steels after treatment was analysed.

INTRODUCTION

In order to reduce weight and save energy, there has been an increasing interest in application of high strength steels for car structural components. As one of the advanced high strength steels, transformation-induced plasticity (TRIP) steels have attracted the attention of both the steelmaking and automotive industries over the last

L.C. Zhang, E.V. Pereloma
School of Mechanical, Materials and Mechatronics Engineering, Faculty of Engineering, University of Wollongong, Wollongong, NSW 2522, Australia
I.B. Timokhina, P.D. Hodgson
Centre for Material and Fibre Innovation, Faculty of Science and Technology, Deakin University, Geelong, Victoria 3217, Australia
A. La Fontaine, S.P. Ringer
Australian Key Centre for Microscopy & Microanalysis, The University of Sydney, NSW 2006, Australia

Paper presented at the 3rd International Conference Thermomechanical Processing of Steels, organised by AIM, Padova, 10-12 september 2008

two decades. TRIP steels consisting of a complex multiphase microstructure (polygonal ferrite, carbide-free bainite, retained austenite and martensite) offer an excellent combination of strength (700–1000 MPa) and ductility (30–40% total elongation) [1]. The interaction of the multiple phases present in the microstructure during deformation and the strain-induced transformation of the metastable retained austenite to martensite [2,3] are thought to be responsible for these mechanical properties. At present, several studies have been undertaken to investigate the effect of the chemical composition and processing parameters of TRIP steel sheets [2,4,5], because these are the two main factors that can affect the volume fraction and stability of the retained austenite in TRIP steels.
On the contrary, little work has been conducted on the variations of the mechanical properties and microstructures during the paint baking of deformed panel parts of TRIP steel sheets. When the steels are used for outer body parts and subjected to the paint baking cycle, additional strengthening of approximately 100–200 MPa arises from bake hardening and results in good shape fix-ability and improved dent and crash resistance [6]. Recently, research on bake hardening of intercritically an-

Steel		C	Mn	Si	Al	Cu	Cr	P
TRIP01	wt.%	0.21	1.68	1.42	0.035	0.010	0.03	0.020
	at.%	0.96	1.67	2.67	0.071	0.009	0.03	0.035
TRIP02	wt.%	0.12	1.39	1.77	0.031	0.005	0.02	0.004
	at.%	0.55	1.38	3.44	0.062	0.004	0.02	0.007

▲
Tab. 1

Chemical composition of the TRIP steels (weight percent, wt.%; atomic percent, at.%).
Composizione chimica degli acciai TRIP (peso percentuale, wt.%; percentuale atomica, at.%).

nealed CMnSi TRIP steels has shown an increase in yield strength and the appearance of yield point after 2–10% pre-straining and baking at 170–180 °C for 20–30 min [4,7]. It has been proposed [4] that the formation of carbide-free bainite is responsible for the increase in the yield strength after bake hardening, because bainite has much faster bake hardening kinetics than the ferrite due to its higher carbon content and smaller grains, reducing the diffusion distances for dislocation locking by carbon.

The present work focused on the effect of pre-straining/bake hardening treatment on the microstructure and mechanical behaviour of intercritically-annealed CMnSi TRIP steels. In particular, the aim was to evaluate the effect of initial microstructure on bake hardening response in the studied steels.

EXPERIMENTAL

Two TRIP steels (hereafter designated as TRIP01 and TRIP02) used in the current work were produced by a standard cold rolling and intercritical annealing processing. The chemical compositions of the studied steels were given in Tab. 1. To study the effect of the pre-straining (PS) and bake hardening (BH) treatment on the mechanical properties, tensile specimens were machined from the strip and subjected to 4–5% pre-straining in tension before bake hardened at 180°C for 30 minutes. Room-temperature mechanical properties of the samples after thermomechanical processing (as-received) and after additional PS/BH treatment were evaluated using an Instron 4500 servohydraulic tensile testing machine with a 100-kN load cell. The crosshead speed was fixed at 0.5 mm/min. Due to the limited amount of material available subsized samples with a 35 mm gauge length and 6 mm width were used. A series of up to three tests were used to define the average values of mechanical properties. The yield strength was defined by the 0.2 % offset stress ($\sigma_{0.2}$) for as-received samples. The bake-hardening response was measured as the strength difference between the upper yield strength after BH treatment and the flow stress after PS [8].

X-ray diffraction analysis was performed using a Philips PW 1130 (40 kV, 25 mA) diffractometer equipped with a monochromator using Cu Kα radiation to confirm the amount of retained austenite in the microstructure. Spectra were taken in the range from 30 to 120 degrees with a 0.02° step size.

The integrated intensities of the $(200)_{\alpha}$, $(211)_{\gamma}$, $(200)_{\gamma}$, $(220)_{\gamma}$, and $(311)_{\gamma}$ peaks were used in the direct comparison method [9]. The carbon concentration of the
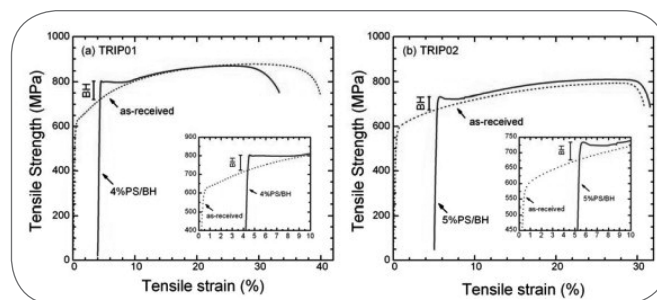
▲
Fig. 1

Uniaxial tensile stress-strain curves of the TRIP steels after different processing.
Curve carico uniassiale -deformazione degli acciai TRIP dopo i diversi processi.

retained austenite was evaluated from the lattice constant measured from the $(200)_{\gamma}$, $(220)_{\gamma}$ and $(311)_{\gamma}$ diffraction peaks using the following equation [10]:

$$a_y = 3.578 + 0.033 \text{ x wt.\%C} \qquad (1)$$

The microstructure was characterised using transmission electron microscopy (TEM) on a Philips CM20 operated at 200 kV and an Imago Scientific Instruments local electrode atom probe (LEAP®). The samples for both studies were cut perpendicular to the deformation (rolling) direction. Thin foils for TEM were prepared by twin jet electropolishing using a solution of 5% perchloric acid in methanol at –20 °C and an operating voltage of 30 V. The dislocation density was calculated by measuring the total dislocation line length in a unit volume of crystal giving a parameter in terms of length (m)/m³. So, the dislocation density (Λ), is given by [11]:

$$\Lambda = 2N_L/Lt, \qquad (2)$$

where N_L is the number of intersections with dislocations, L the length of random lines, and t the foil thickness. The standard two-stage electropolishing procedure was used to prepare the needle-shaped atom probe specimens [12]. Atom probe experiments were performed on a local electrode atom probe located at the University of Sydney, with a sample temperature of 80 K, a pulse repetition rate of 200 kHz, and a pulse fraction of 0.2. Maximum separation envelope method [12] with d_{max} = 1 nm was utilised to identify C segregation to dislocations, clusters and fine precipitates in polygonal ferrite or bainitic ferrite.

Steel	Conditions	UTS (MPa)	YS (MPa)	Total El (%)	Uniform El (%)	BH response (MPa)
TRIP01	as-received	880 ± 15	608 ± 20	40 ± 2	30 ± 2	N/A
	4%PS/BH	891 ± 15	803 ± 20	29 ± 2	21 ± 2	82 ± 2
TRIP02	as-received	795 ± 10	520 ± 10	31 ± 2	27 ± 3	N/A
	5%PS/BH	810 ± 8	735 ± 5	27 ± 2	21 ± 3	60 ± 3
UTS: ultimate tensile strength, YS: yield strength, Total El: total elongation, Uniform El: uniform elongation, BH response: bake hardening response.						

▲
Tab. 2

Mechanical properties of the investigated TRIP steels after different processing.
Proprietà meccaniche degli acciai TRIP investigati dopo i diversi processi.

RESULTS

A. Mechanical properties

The mechanical properties of the steels in both as-received and PS/BH state are given in Fig. 1 and Tab. 2. Both steels exhibited a good combination of strength and ductility in the as-received condition with higher values of strength and ductility for TRIP01 steel compared with the TRIP02 (Tab. 2). In this state both steels showed a continuous yielding behaviour (Fig. 1). A continuous exponential decrease was distinct in the strain-hardening rate curves for both steels (Figs. 2 (a) and (b)). After the PS/BH treatment, both steels demonstrated a yield-point phenomenon on the stress-strain curves. After yield point elongation, the
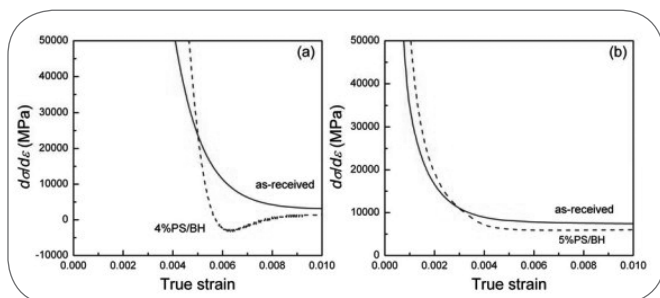

▲
Fig. 2

Variations of the strain hardening rate with the true strain of the (a) TRIP01 and (b) TRIP02 steels.
Variazioni della velocità di incrudimento con la sollecitazione negli acciai (a) TRIP01 e (b) TRIP02.
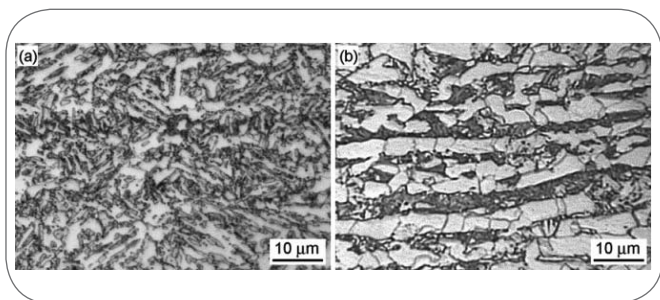

▲
Fig. 3

Optical micrographs of the (a) TRIP01 and (b) TRIP02 steels after PS/BH treatment.
Micrografie ottiche degli acciai (a) TRIP01 e (b) TRIP02 dopo trattamento di PS/BH.

flow stress started to increase until necking occurred.
The strain-hardening rate curve of the TRIP02 steel after PS/BH treatment still showed a continuous exponential decrease (Fig. 2(b)). On the contrary, the strain-hardening rate of the TRIP01 steel after PS/BH treatment decreased sharply to negative values and then started to increase at around 6.5% true strain (Fig. 2(a)). As seen from Tab. 2, the PS/BH treatment led to a significantly higher yield strength (~200 MPa) and a slightly higher ultimate tensile strength (~15 MPa) in both steels. However, the total elongation decreased by ~11% and ~4% for the TRIP01 and the TRIP02 steels, respectively, and the uniform elongations reduced by ~9% for TRIP01 and ~6% for the TRIP02. Both TRIP steels displayed a noticeable bake-hardening response (~82 and ~60 MPa for the TRIP01 and the TRIP02, respectively).

B. Microstructural features

Optical micrographs revealed that both TRIP steels showed a complex multiphase microstructure (Fig. 3). In the as-received condition, the microstructure of the TRIP01 steel consisted of ~ 30 ± 3% polygonal ferrite (PF), ~56 ± 3% bainite, ~10 ± 3% retained austenite (RA) with an average carbon content of 1.21 ± 0.04 wt.% and the remaining of martensite. The polygonal ferrite grain size was 3 ± 1.5 μm. The TRIP02 steel contained ~70 ± 3% polygonal ferrite and ~20 ± 3% retained austenite with an average carbon content of 1.20 ± 0.05 wt.%. The remaining small volume fraction contained martensite and bainite. The average size of polygonal ferrite grains was 4 ± 1.5 μm. The volume fraction of retained austenite decreased from ~10% in as-received condition to ~8% in PS/BH state for the TRIP01 and from ~20% in the as-received condition to ~12% in the PS/BH state for the TRIP02 steel. In addition, the PS/BH treatment led to an increase in carbon content of retained austenite to 1.28 ± 0.04 wt.% (TRIP01) and 1.30 ± 0.03 wt.% (TRIP02). It is noted that bainitic ferrite grains in the TRIP02 were predominantly long and parallel laths while those in the TRIP01 steel had random orientation.
Fig. 4 illustrated a more detailed microstructure of the steels after different processing. The microstructure in the as-received state was composed of polygonal ferrite, carbide-free bainite, retained austenite and martensite (Figs. 4 (a) and (b)). After the PS/BH treatment, a lot of dislocations were observed in the polygonal ferrite, as seen from Figs. 4 (c) and (d). The most affected regions of PF grains were in the vicinity of martensite or retained austenite crystals, as denoted by the black arrows. At the same time, the formation of dislocation cells in the polygo-
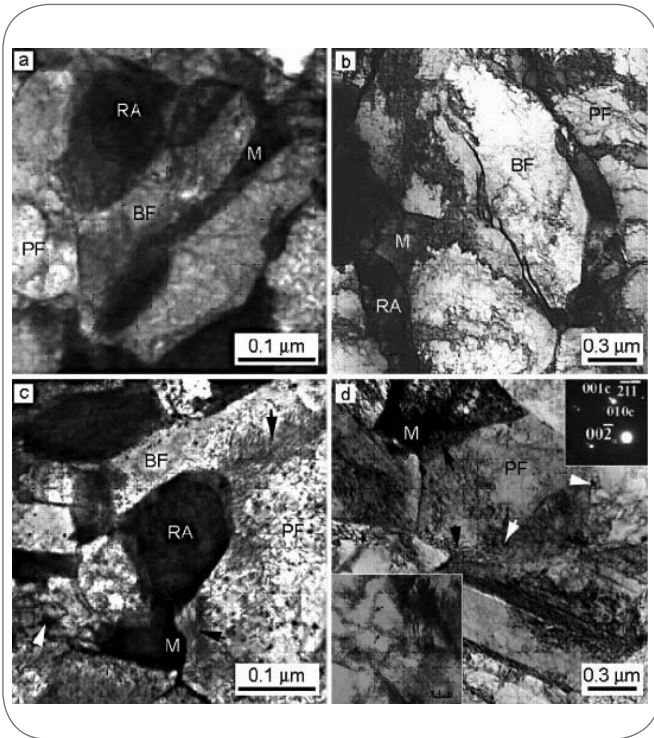
Bright field TEM images of the (a) TRIP01 and (b) TRIP02 steels in the as-received condition, and (c) TRIP01 and (d) TRIP02 after PS/BH treatment. PF: polygonal ferrite, RA: retained austenite, BF: bainitic ferrite, and M: martensite. Black arrows denote localised regions of increased dislocation density and white arrows indicate carbides. Inset: right-top – selected area diffraction pattern of iron carbide in BF [112]$_\alpha$ // [100]$_c$; bottom-left – cell structure in PF.

4 Immagini TEM in campo chiaro degli acciai (a) TRIP01 e (b) TRIP02 nella condizione come ricevuti, e degli acciai (c) TRIP01 e (d) TRIP02 dopo trattamento PS/BH. PF: ferrite poligonale, RA: austenite residua, BF: ferrite bainitica, e M: martensite. Le frecce nere indicano regioni localizzate con aumento della densità di dislocazioni; le frecce bianche indicano i carburi . Riquadri: in alto a destra– figure di diffrazione, in area selezionata, di carburo di ferro in BF [112]$_\alpha$ // [100]$_c$; in basso a sinistra– struttura cellulare in PF.

nal ferrite was also observed (Fig. 4 bottom-left inset). In addition, some small iron carbides were visible in the bainite ferrite, as denoted by white arrows in Figs. 4 (c) and (d) and the selected area diffraction pattern (SAED) in the right-top inset in Fig. 4 (d). The PS/BH treatment led to an increase in the average dislocation density of polygonal ferrite from 1.75×10^{-14} m^{-2} to 2.7×10^{-14} m^{-2} for the TRIP02 steel [7]. In addition, numerous iron carbides were apparent in the martensite after PS/BH treatment (Fig. 5).

## C. Atom probe tomography (APT) characterisations

APT was used to study the partitioning of carbon and other alloying elements and solute segregation in the different phases in the as-received condition and after the PS/BH treatment. In this study, the phases were dis-
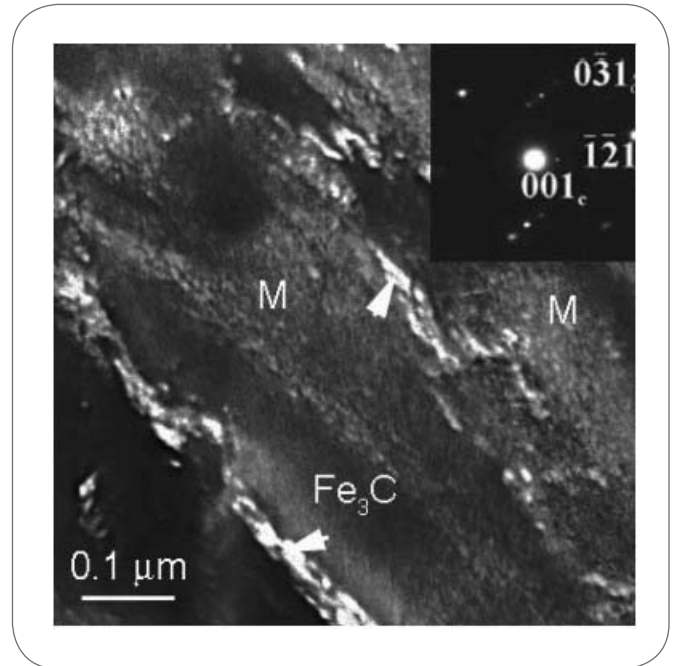
Dark field TEM image and corresponding selected area diffraction pattern of the carbide formation in martensite in the zones axis of [113]$_\alpha$ // [$\bar{2}$ 10]$_c$ in the TRIP02 steel after PS/BH treatment. M: martensite.

Immagini TEM in campo scuro e corrispondente figura di diffrazione in area selezionata della formazione di carburi nella martensite nell'asse delle zone [113]$_\alpha$ // [$\bar{2}$ 10]$_c$ nell'acciaio TRIP02 dopo trattamento PS/BH. M: martensite.

tinguished based on their carbon content, i.e. < 0.07 at.% was polygonal ferrite, 0.1–0.3 at.% bainite and >2 at.% martensite or RA [13]. In the as-received condition, the formation of three main regions in the microstructure
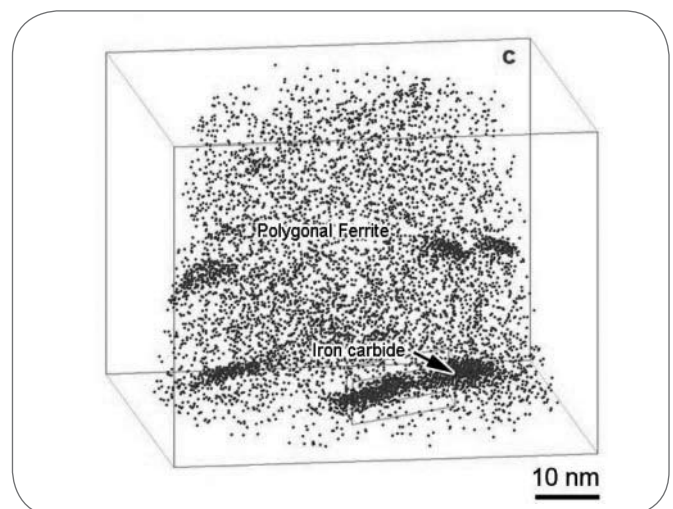
Carbon atom map of as-received TRIP01 steel.

Mappa dell'atomo di carbonio nell'acciaio TRIP01 come ricevuto.

Steel	Phase		Concentration		
			C	Si	Mn
TRIP01	Polygonal ferrite		< 0.003	4.02±0.01	1.26±0.01
	Bainitic ferrite after PS/BH		0.11±0.01	3.30±0.1	1.44±0.04
	Martensite		3.22±0.01	3.61±0.01	2.28±0.01
TRIP02	Polygonal ferrite		0.02±0.01	3.90±0.03	0.90±0.03
	Retained austenite		4.60±0.02	3.90±0.05	1.02±0.03
	Bainite	Bainitic ferrite	0.20±0.03	2.80±0.02	1.50±0.02
		Retained austenite	5.10±0.20	4.40±0.05	1.20±0.03

▲
Tab. 3

Concentrations of the major alloying elements (at.%) in the phases of as-received steels, except where indicated otherwise, determined using APT and calculated based on the number of atoms.
Concentrazioni dei maggiori elementi alliganti (at.%) nelle fasi degli acciai come ricevuti, ad eccezione di dove diversamente indicato, determinati utilizzando APT e calcolati sulla base del numero di atomi.

of both steels was detected: (i) carbon-depleted region with an average carbon content of between 0.003 at.% and 0.02 at.% (Figs. 6 and 7), (ii) a carbon-enriched region with average carbon content of between 3 at.% and 5.5 at.% (Fig. 7), and (iii) a volume or region, which can be described as a mixture of carbon-enriched (5.10 ± 0.20 at.%) and carbon-depleted (0.20 ± 0.03 at.%) regions (Fig. 7). A summary of their major elemental concentrations is given in Tab. 3. Therefore, from this the first region was polygonal
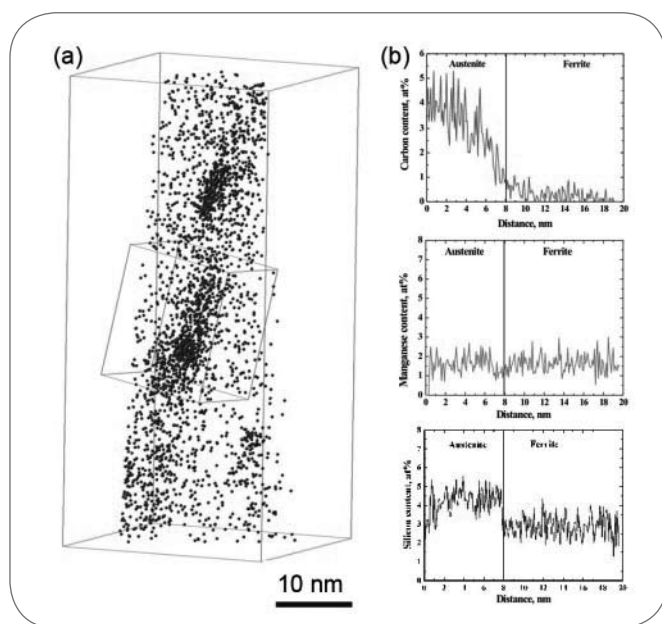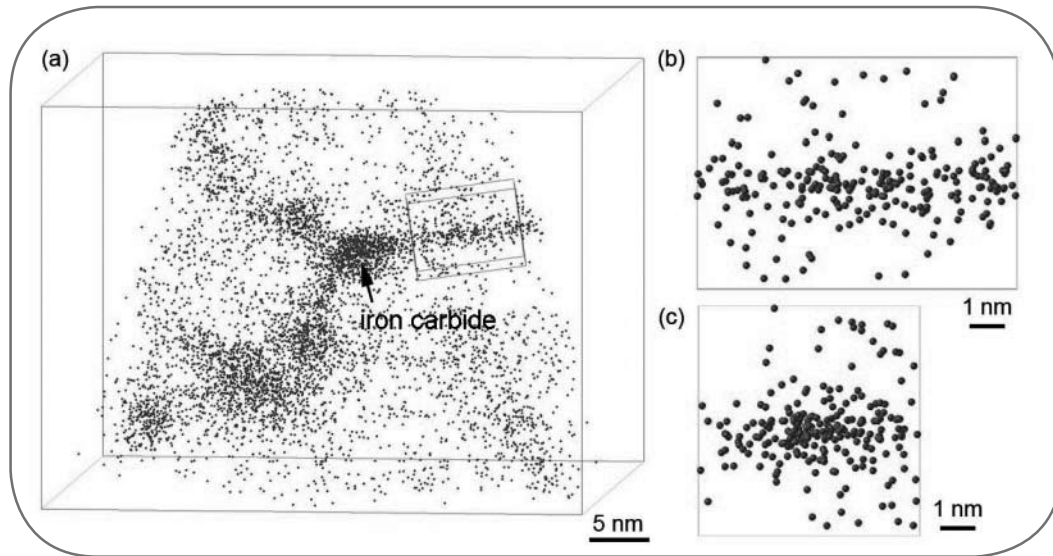

▲
Fig. 7

(a) Carbon atom map of as-received TRIP02 sample showing bainitic ferrite and retained austenite and (b) C, Mn and Si compositional profiles across along green (nearly horizontal) line of selected box shown in (a).
Mappa dell'atomo di carbonio del campione di acciaio TRIP02 come ricevuto che mostra ferrite bainitica e austenite residua e (b) profili di composizione di C, Mn e Si lungo la linea verde (quasi orizzontale) del riquadro selezionato mostrato in (a).

ferrite, the second retained austenite or martensite, and the third region was bainite, where the carbon-rich region was retained austenite/martensite and the carbon-depleted region was bainitic ferrite. In both steels the Si content of polygonal ferrite was higher than the nominal Si content while the Mn content was lower (Tab. 3). In addition, small iron carbide particles appeared in the as-received TRIP01 steel (Fig. 6). As shown in the APT map of the as-received TRIP02 steel (Fig. 7), the retained austenite crystals may appear in bainite, which had a plate-like shape with a thickness of 16 ± 2 nm (Fig. 7) and contained a high carbon content (Tab. 3). The bainitic ferrite was characterised by a significantly higher carbon content (~0.2 at.%), lower Si content (~2.8 at.%) and higher Mn level (~1.5 at.%) than polygonal ferrite (Tab. 3). The bainitic ferrite in the TRIP01 steel after PS/BH treatment had higher than expected Si content (Tab. 3). This might be associated with the decomposition of bainitic ferrite during bake hardening resulting in the formation of iron carbides and rejection of Si back into the BF matrix (Fig. 8).

After the PS/BH treatment, the formation of Cottrell atmospheres at dislocations in the polygonal ferrite and bainitic ferrite was evident from the atom probe maps (Figs. 8). The rod-like shape of carbon segregation to dislocations is clear from two atom maps taken in perpendicular directions (Figs. 8 (b) and (c)). It is also clear from Fig. 8 (a) that C segregation was non-uniform along the dislocations forming a complex tangle, with the formation of iron carbides at dislocation intersections. The carbon concentration in the core of the atmosphere reached up to ~7 at.%. At the same time, concentration profiles across the coarsest carbides revealed a carbon content at the centre of ~21 at.% which is close to the level in Fe_3C. Carbon segregations to the particular plane in the coarse retained austenite crystals were observed in the TRIP02 after PS/BH (Fig. 9 (a)). The angle between the saturated planes was ±35°. The compositional profiles across these planes showed the carbon enrichment to 7±0.08 at.%, while Si and Mn concentrations were similar to the matrix composition (Fig. 9 (b)).
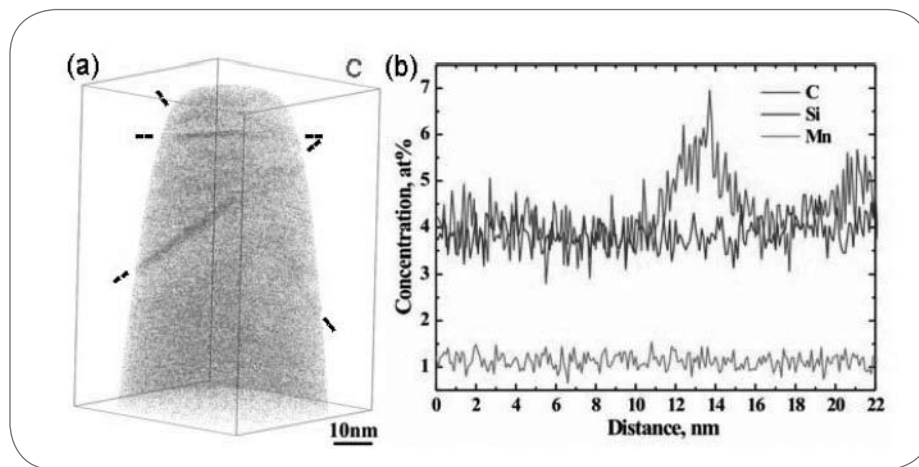
DISCUSSION

Both steels showed continuous yielding in the as-received condition, while they exhibited a yield-point phenomenon

▲
Fig. 8

(a) Carbon atom map of carbon segregation and iron carbides, and (b) and (c) representative selected C atom maps of a Cottrell atmosphere from two perpendicular directions of the TRIPO1 steel after PS/BH treatment.
(a) Mappa dell'atomo di carbonio relativa alla segregazione di carbonio e ai carburi di ferro, e (b) e (c) mappe rappresentative dell'atomo C selezionate di un'atmosfera di Cottrell da due direzioni perpendicolari per l'acciaio TRIPO1 dopo trattamento PS/BH.

ultimate tensile strength (10–15 MPa), accompanied by the reductions in both total and uniform elongations (Tab. 2). It has been suggested that this is a result of martensite and bainite strengthening effect. The bake-hardening effect could be related to the microstructural changes taking place during the pre-straining/bake-hardening treatment. The main changes were: (i) a decrease in the volume fraction of retained austenite; (ii) an increase in the average dislocation density of polygonal ferrite; (iii) the formation of cell substructure in the polygonal ferrite; (iv) a localised increase in the dislocation density of the polygonal ferrite regions adjacent to martensite/RA; and (v) the formation of fine iron carbides in bainite and martensite. According to the stress fields of the dislocations [14], a rapid stress-induced ordering of solute carbon atoms can take place easily into preferred positions in iron carbides during straining, and the carbon atoms could migrate towards the dislocation under straining. Thereafter, at the bake-hardening temperature additional carbon atoms would be able to migrate to the dislocations to form clusters or fine particles. This was proved by both TEM and APT observations (Figs. 4 (c) and (d) and Fig. 8), where plenty of iron carbides were visible in after PS/BH treatment. The precipitation of iron carbides resulted in an increase in strength but a reduction of ductility. Moreover, the additional effect of the increased dislocation density near PF/RA or PF/M interfaces should be considered. In general, the yielding point on stress-strain curves occurs as a result of unlocking the dislocations from Cottrell atmospheres by a high stress or for case of a strong pinning by fine precipitates, by creating new dislocations. As seen from Fig. 8, there is strong evidence of Cottrell atmospheres in the TRIP01 steel after PS/BH treatment.

Together with the presence of a local minimum on the strain-hardening rate curve in the Fig. 2(a), this indicates that dislocation unlocking process is responsible for the observed yield point drop in the TRIP01 steel. This is not a case for the TRIP02 steel, as strain-hardening rate curve shows continuous exponential decrease. Thus, yield point

on the stress-strain curves after PS/BH treatment (Fig. 1). However, the strain-hardening rate of the TRIP01 steel after PS/BH treatment displayed the transition from continuous to discontinuous strain-hardening behaviour; whereas the strain-hardening curve of the TRIP02 steel still showed a continuous behaviour similar to the as-received condition (Fig. 2). Both steels demonstrated sufficient bake-hardening response and a slight increase in the

phenomenon in TRIP02 is associated with the increase of the number of mobile dislocations due to the generation of the new ones. This difference in steels behaviour is due to the main microstructural difference of both steels. As seen from Fig. 3, there was about 70% polygonal ferrite in the TRIP02, in which numerous new dislocations easily formed during pre-straining, as well as during tensile testing of pre-strained and bake-hardened samples. There was much less polygonal ferrite (~30%) and much more bainite (~56%) in TRIP01, which was not as susceptible to pre-straining as PF and in which the formation of Cottrell atmospheres took place [4].

CONCLUSIONS

A pre-straining and bake hardening treatment led to a significant strength increase in CMnSi TRIP steels with some reduction in ductility. The observed effects of pre-straining and bake hardening on the mechanical behaviour of the steels were associated with the main changes in their microstructure: microstructural changes in polygonal ferrite, such as an increase in the dislocation density and the formation of cell substructure, a localized increase of the dislocation density in the polygonal ferrite regions adjacent to martensite and the formation of fine precipitation in bainite and martensite. It was concluded that the observed yield point phenomenon was due to dislocation unlocking in the TRIP01 steel, which contained bainite as a dominant phase. Contrarily, formation of new mobile dislocations was the reason for the yield drop in TRIP02 steel, in which polygonal ferrite was a major phase.

ACKNOWLEDGEMENT

REFERENCES

1] Y. SAKUMA, O. MATSUMURA and H. TAKECHI, Metall. Mater. Trans. A 22 (1991), p.489.
2] P.J. JACQUES, J. LADRIÈRE and F. DELANNY, Metall. Mater. Trans. A, 32 (2001), p.2759.
3] V.F. ZACKAY, E.R. PARKER, D. FAHR and R. BUSH, Trans. ASM, 60 (1967), p.252.
4] B.C. DE COOMAN, Curr. Opin. Solid State Mater. Sci. 8 (2004), p.285.
5] D.V. EDMONDS, K. HE, F.C. RIZZO, B.C. DE COOMAN, D.K. MATLOCK, and J.G. SPEER, Mater. Sci. Eng. A 438-440 (2006), p.25.
6] L.J. BAKER, S.R. DANIEL and J.D. PARKER, Mater. Sci. Tech. 18 (2002), p. 355.
7] I.B. TIMOKHINA, P.D. HODGSON and E.V. PERELOMA, Metall. Mater. Trans. A 38 (2007), p.2442.
8] A.K. DE, S. VANDEPUTTE and B.C. DE COOMAN, Scripta Mater. 44 (2001), p.695.
9] B.D. CULLITY, Elements of X-ray diffraction, Addison-Wesley, London (1978) p.411.
10] D.J. DYSON and B. HOLMES, Iron Steel Inst. 208 (1970), p.469.
11] P.B. HIRSCH, R.B. NICHOLSON, A. HOWIE, D.W. PASHLEY and M.J. WHELAN, Electron microscopy of thin crystals, Butterworths, London (1965), p. 51.
12] M.K. MILLER, Atom Probe Tomography, in: Handbook of Microscopy for Nanotechnology, eds. N. YAO and Z.L. WANG, Kluwer Academic Press, New York (2005), p.236.
13] E.V. PERELOMA, I.B. TIMOKHINA, M.K. Miller and P.D. HODGSON, Acta Mater. 55 (2007), p.2587.
14] D. KALISH and M. COHEN, Mater. Sci. Eng. 6 (1970), p. 156.

ABSTRACT

EFFETTO DI PRE-TENSIONAMENTO E BAKE-HARDENING SULLA microstruttura E SULLE PROPRIETA' MECCANICHE E DI UN ACCIAIO TRIP CMnSi

Parole chiave: acciaio, deformazioni plastiche, proprietà

Nel lavoro sono stati studiati gli effetti di pre-tensionamento e bake hardening sul comportamento meccanico e sui cambiamenti microstrutturali in due acciai CMnSi TRIP (TRansformation-Induced Plasticity) con diverse microstrutture dopo ricottura intercritica. L'acciaio TRIP, prima e dopo i processi di pre-tensionamento e bake-hardening, sono stati caratterizzati mediante diffrazione a raggi X, microscopia ottica, microscopia elettronica a trasmissione, sonda atomica tridimensionale e prove a trazione. Entrambi gli acciai hanno mostrato comportamento discontinuo allo snervamento e un significativo aumento della resistenza neccanica con una riduzione della duttilità dopo il trattamento di pre-tensionamento e bake-hardening. I seguenti principali cambiamenti microstrutturali sono responsabili dei comportamenti meccanici osservati una diminuzione della frazione in volume di austenite residua, un aumento della densità delle dislocazioni e la formazione di una sottostruttura a celle nella ferrite poligonale, una maggiore densità di dislocazioni localizzata nelle regioni a ferrite poligonale adiacenti alla martensite o all'austenite residua, una precipitazione di carburi di ferro nella bainite e nella martensite.

Infine è stato analizzato il meccanismo relativo alla fenomenologia connessa al limite di snervamento osservato in entrambi gli acciai dopo trattamento.